

# Spatially self-organized resilient networks by a distributed cooperative mechanism

Yukio Hayashi <sup>a</sup>,

<sup>a</sup>*Japan Advanced Institute of Science and Technology, Ishikawa 923-1292, Japan*

---

## Abstract

The robustness of connectivity and the efficiency of paths are incompatible in many real networks. We propose a self-organization mechanism for incrementally generating onion-like networks with positive degree-degree correlations whose robustness is nearly optimal. As a spatial extension of the generation model based on cooperative copying and adding shortcut, we show that the growing networks become more robust and efficient through enhancing the onion-like topological structure on a space. The reasonable constraint for locating nodes on the perimeter in typical surface growth as a self-propagation does not affect these properties of the tolerance and the path length. Moreover, the robustness can be recovered in the random growth damaged by insistent sequential attacks even without any remedial measures.

*Key words:* Self-Organization; Robust Onion-like Structure; Fractal Surface Growth; Cooperative Multiplexing; Resilient System

---

## 1 Introduction

In modern society, our daily activities depend on energy supply, communication, transportation, economic, and ecological networks, however their infrastructure systems are complex and not constructed by a central control. Unfortunately, natural and man-made disasters occur at many locations in the world, sometimes they bring to the crises of such network infrastructures. For the improvements with robust connectivity, it is expected to study the admirable self-organizations appeared in natural and social systems [1]. In particular, several fundamental mechanisms: preferential attachment [2], copying [3,4], survival [5,6,7], subdivision (fragmentation) [8,9,10,11,12,13], or aggregation [13,14] are attractive for generating networks in the interdisciplinary research fields of physics, biology, sociology, and computer science.

With the break of complex network science in the beginning of 21st century, it is well known that in many social, technological, and biological networks there exists a common *scale-free* (SF) structure whose power-law degree distribution is generated by the preferential attachment [2] likened to “rich-get-richer” rule. The SF networks have the efficient *small-world* (SW) property [15] that the path length counted by the hops through minimum intermediate nodes between any two nodes is short even for a large network size, however they also have an extreme vulnerability against intentional attacks in spite of having the tolerance of connectivity against random failures [16]. The vulnerability comes from a few existing of large degree hub nodes in a power-law distribution. Thus, the efficiency of path and the robustness of connectivity are incompatible in many real networks, such as Internet, power-grids, airline networks, metabolic networks, and so on. If we do not persist the generation mechanism of real

networks, we may find other more desirable mechanism to maintain both the robustness and the efficiency.

Since the natural design methods are not limited to only the selfish rule for a good network in efficiency, scalability, stability, adaptivity, or other criteria, we consider a random copying process to generate complex networks as one of other candidates for the design of future network infrastructure. We take into account self-propagation in maintaining the robust network structure without degrading the communication or transportation performance in the growth. Although the duplication process has been so far considered to be fundamental in a model of protein-protein interaction networks [3,4], its generation mechanism with some modifications may be applied to a self-organized design of social and/or technological networks in urban planning, civil engineering, or information system science.

On the other hand, by numerical and theoretical analysis, it has been shown that [17,18,19] onion-like topological structure with positive degree-degree correlations gives the optimal robustness against targeted attacks to hub nodes in an SF network. For any degree distribution, the onion-like topology consists of a core of highly connected nodes hierarchically surrounded by rings of nodes with decreasing degree. In a related generation method in a family of SF networks, a deterministic model called as *mandala network* that consist of recurrently expanded intra- and inner-connections of ringed nodes has been studied [20]; the robustness is improved by rewiring or adding links applied to the outmost two rings of nodes from the core of connected hub nodes. Furthermore, an efficient rewiring algorithm has been developed for generating a network of onion-like topology with the nearly optimal robustness under a given degree distribution [21]. However, these constructions are based on

swapping endpoints of randomly chosen two links [17,18], expanding the rings by simultaneously adding  $n_i = 2n_{i-1}$  nodes for the  $i$ -th iterations [20], and entirely rewiring of links [21] like a configuration model [22], an incremental generation method was not found for the networks with onion-like topology. Recently, an incrementally growing method of such networks with onion-like topology has been proposed [23] as a modification of the *duplication-divergence* (D-D) model [3,4] in enhancing the degree-degree correlations.

In this paper, we focus on a self-organized design for infrastructural communication and transportation network systems on a space, rather than the detail technologies and facilities. In particular, we consider a spatial growth of network with the robust onion-like topology. Although there are many types of failures and attacks, e.g. locally spreading damages in a disaster, this paper treats typical random and targeted removal of nodes for investigating the fundamental property of robustness. Instead, we take notice of the uncertainty: whether the robust structure can be maintained or not in a spatial growing of network, because the embedding on a space imposes some kind of constraints on the construction of network topology. The organization of this paper is as follows. In Sec. 2, we introduce a biologically inspired basic model [23] for generating onion-like topological structure with strong robustness. Without loss of the robust onion-like topology, we extend it to spatial networks according to surface growth. Such growth gives a hint for finding plausible self-propagation mechanism in distributed network systems. In Sec. 3, we show good properties for the robustness of connectivity and the efficiency of path on the growing networks. In particular, it is attractive that the reasonable constraint on a contact area of surface for locating nodes in the growth does not affect these properties of robustness and efficiency. Moreover, we show the resilient connec-

tivity. Even without any remedial measures, the robustness can be recovered in the growth damaged by sequential attacks. Resilience [24] is an important concept to heal over, repair, and recover the performance from a damaged system, the recovery of robustness will give a first step to develop resilient network systems. Some strategies for the resilient networks are discussed particularly in interdependent networks [25,26] recently. In Sec. 4, we summarize these results, and mention several issues to make a more resilient network system.

## 2 Spatially growing onion-like networks

### 2.1 Basic generation procedures

This subsection introduces a basic model of incrementally growing networks with onion-like topology [23]. In the next subsection, we extend it to a spatial model and explain how to locate a node on a space.

In the conventional D-D model [3,4], as the duplication process, a new node added per time step links to connected neighbor nodes of a randomly chosen node. Then deletion of the duplication links occurs with probability  $\delta$ . We modify the duplication process by non-trivial discovering ideas; the differences of our proposed network [23] from the D-D model are the adding of a mutual link between new and randomly chosen nodes, and the simultaneous progress of copying and adding shortcut links at a time-interval to enhance the onion-like topological structure. We call the combination of a mutual link and duplication links as copying. Shortcut means an analogy to random connections in the SW model [15]. The outline of network generation consists of (1)

At each time step, a new node is added at a position on a square lattice. (2) As the copying process, the new node stochastically links to connected neighbor nodes of a chosen node limited on the perimeter (surface) of a spatially growing network. (3) In order to enhance the robustness of connectivity, we consider having positive degree-degree correlations in the copying and adding of shortcut links. These procedures are summarized as follows.

**Step 0** Set an initial configuration of connected  $N_0$  nodes.

**Step 1** At each time step  $t = 1, 2, \dots$ , a new node is added on a space. As shown to the topological structure in Fig. 1(a), the new node  $i$  connects to a randomly chosen node and to the neighbor nodes  $j$  with a probability  $(1 - \delta) \times p$  [21],

$$p \stackrel{\text{def}}{=} \frac{1}{1 + a |k_i - k_j|}, \quad (1)$$

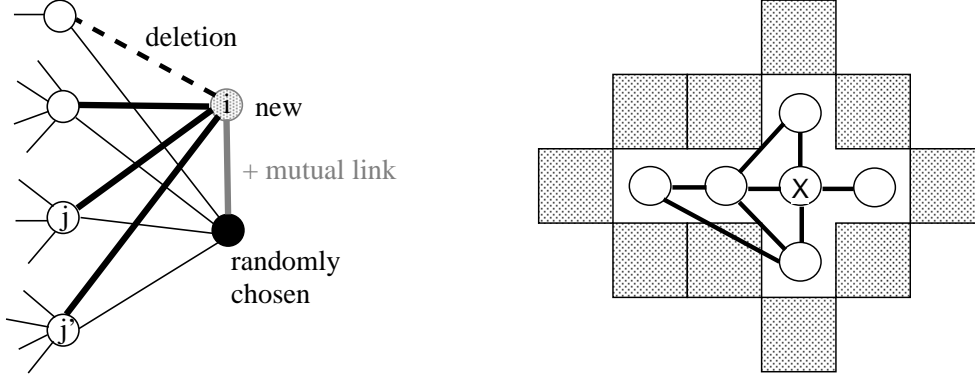
where  $\delta$  is a rate of link deletion,  $a \geq 0$  is a parameter, and  $k_i$  and  $k_j$  denote the degrees of nodes  $i$  and  $j$ . Since the linking is a stochastic process for the new node  $i$ , unknown  $k_i$  in Eq.(1) is anticipatorily set as  $(1 - \delta) \times$  the degree of the chosen node.

**Step 2** Moreover, at every time-interval  $IT$ , shortcut links until the number  $p_{sc}M(t)$  are added between randomly chosen nodes  $i$  and  $j$  according to the probability of Eq.(1) in prohibiting self-loops at a node and duplicate connections between two nodes<sup>1</sup>. Here,  $p_{sc}$  is a rate of adding shortcut links,  $M(t)$  denotes the number of links in the network at that time  $t = IT, 2IT, 3IT, \dots$ , and  $IT$  is defined by time steps greater than one.

**Step 3** The above processes in Steps 1 and 2 are repeated up to a given size  $N$  for  $N(t) = t + N_0$ .

---

<sup>1</sup> In the prohibitive case, selections of other nodes are tried in the same way.



(a) Copying process

(b) Candidates of node's location

Fig. 1. Basic topological and spatial processes. (a) Thick black and gray lines show the generated links by the copying process. Then deletion of dashed line occurs with probability  $\delta \times p$ . Thin lines show the already existing links. We remark that such a bypath of nodes  $j'$ - $i$ - $j$  is created for the path of nodes  $j'$ -chosen- $j$ . (b) Open circles are selectable nodes, but one with cross mark is not. Shaded sites show the perimeter as inserted locations of a new node.

We emphasize the following effects of copying and shortcut on the robustness.

- Local proxy function: by copying to make bypaths via another access point of new node (see Fig. 1(a)) as a duplexing and the accumulated multiplexing via other new nodes in the growth
- Complementary function: by adding shortcut links especially between small degree (homophily) nodes to enhance the robustness

Note that the local redundancy with bypaths is often used in distributed computer communication systems. Our generation method is based on a co-operation mechanism that consists of the above functions and the linking of similar degree nodes as homophily. Each part constructed by the copying and adding shortcut links helps each other with the division of roles to be a robust network in taking into account positive degree-degree correlations. More precisely, we explain the roles as follows. Since the double random selections

for the neighbor nodes  $j$  contribute to an equivalent effect of preferential attachment [27,28], large degree nodes  $i$  and  $j$  tend to be connected together when the chosen node has a large degree. However, such positive correlations between small degree nodes are weak in the tree-like structure generated by only the copying process [23]. Thus, in order to make an onion-like topological structure, we further consider addition of shortcut links [15] between randomly chosen nodes  $i$  and  $j$  with the probability of Eq.(1). The adding per a time-interval  $IT$  instead of each time step is considered as non-dominant (complementary) but necessary process for generating an onion-like topology. It has already been shown that adding some shortcut links between randomly chosen nodes improves the robustness in the theory for the small-world model [29] and also in the numerical simulations for geographical networks: random Apollonian networks [30], multi-scale quartered networks [31], and link survival networks [7]. In addition, positive degree-degree correlations tend to appear in randomly growing networks [32]. Therefore, in our network grown by the simultaneous progress of the copying and adding shortcut links, it is expected that the robustness becomes stronger due to enhancing positive degree-degree correlations for emerging the onion-like topology.

## *2.2 Spatial networks generated by surface growth with robustness*

In this subsection, we explain how to locate a new node in the network according to typical models of surface growth.

There exist many complex pattern-formations far from equilibrium in nature [33] as living open systems. Several models of fractal growing random pattern have been studied for the growth of biological cell colonies, fluid displacing in



a porous medium, dendritic solidification, dielectric breakdown, snowflake formation, and bacterial colonies [33,34]. Some most important classes of surface growth include *Diffusion-Limited Aggregation* (DLA) [35,36], *Invasion Percolation* (IP) [37], and *Eden growth* [38], which can be used as a basis for understanding a wide range of pattern-formation phenomena with disorderly growth.

Thus, we consider diffusively growing networks on surface with both onion-like topological and fractal spatial structures. In our network, the position of new node is determined by DLA, IP, and Eden models on a square lattice. Exactly, only DLA and IP models at the critical threshold generate a fractal structure. These models have the following processes [33] and explanations to give a new insight of the self-organized design of spatial network.

**DLA model** As an idealization of the irreversible aggregation, the following process forms a growing diffusive cluster. It is motivated from several phenomena of biological interest for the surface growth with complicated shape, which corresponds to a distributed local extension of technological or social network system.

The initial configuration is a single occupied site on a lattice. At each generation step, the cluster of occupied sites is grown by launching a random walker from outside of the occupied region, and allowing it to its random walk path until it reaches a site that is adjacent to the occupied site. The process is repeated with a new random walker.

**IP model** It is based on a transport process by the slow displacement of a wetting fluid in a porous media. The percolation growth corresponds to an extension in avoiding geographical obstacles engraved by longstanding rains and winds for the network construction.

Initially, random numbers or thresholds are assigned to the sites of a lattice. They represent the capillary pressures for penetrating through the porous medium or the difficulties (low priorities) to install network connections on a geographical space. At each generation step, an unoccupied site with the lowest threshold (smallest random number, highest priority) is selected as an injection point on the perimeter, and occupied. Such process is repeated.

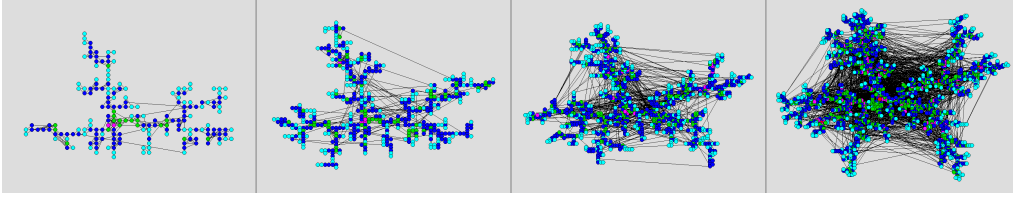
**Eden model** It imitates a cell division process, which corresponds to the most local extension to neighbor space in a simple way.

Starting with an occupied cell (site), an occupied cell on the perimeter of the cluster is randomly selected with equal probability. One of its nearest neighbor unoccupied perimeter cell is selected and occupied. The cluster is grown by adding the selected nearest neighbor at each generation step. Such process is repeated for a new selection of cell with the division.

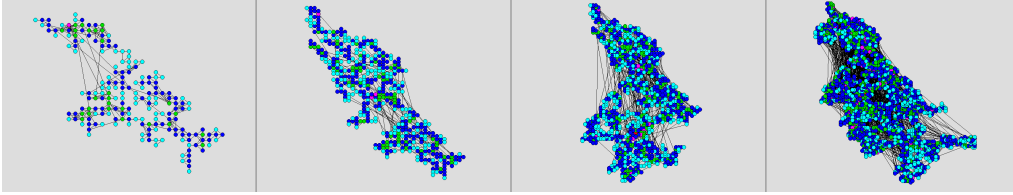
As a constraint in the surface growth, the inserted position of new node is limited on the perimeter of connected cluster. Figure 1(b) shows that the internal node(s) marked by  $\times$  can't be selected, since the only neighbors marked by  $\bigcirc$  of shaded positions are the candidates. In other words, the selection of a node is not uniformly at random (u.a.r) in the growing network. However, the limitation is rather reasonable, since the perimeter is a contact area from the outer world into the network through the growth. Moreover, although u.a.r selection is not equivalent to independent one, the perimeter sites can grow simultaneously in distributed processes on several places. These sites autonomously perform the processes initiated by diffusive growing, own local timers corresponded to thresholds<sup>2</sup>, or random numbers. It is an important

---

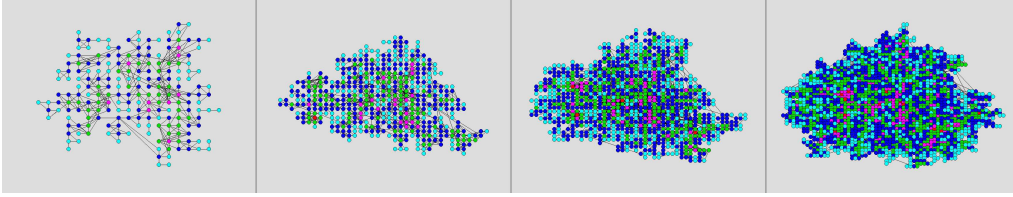
<sup>2</sup> The threshold may be related to the amount of potential communication or transportation requests which are proportional to a population density.



(a) DLA Model:  $\delta = 0.3$ ,  $p_{sc} = 0.015$



(b) IP Model:  $\delta = 0.3$ ,  $p_{sc} = 0.013$



(c) Eden Model:  $\delta = 0.3$ ,  $p_{sc} = 0.009$

Fig. 2. (Color online) Growing spatial networks for  $N(t) = 200, 500, 1000$  and  $2000$  from left to right with arranged scales. Gradually colored node is according to its degree: 1-3(cyan), 4-6(blue), 7-9(green), 10-12(magenta), and the larger(red). discussion point in this paper whether the constraint on the surface growth hardly affect the emergence of an onion-like topological structure.

Typical shapes of the growing spatial networks are shown in Fig. 2. These models form (a) dendritic, (b) porous, and (c) compact patterns, respectively, on a square lattice. Large degree (magenta and red) nodes are spontaneously interspersed in constructing densely connected parts. The rate  $p_{sc}$  of adding shortcut links is regulated to be a same condition of the connection density as  $\langle k \rangle \approx 5.6$  at  $N = 2000$  in all models. We also set initial complete graph of  $N_0 = 4$ ,  $IT = 50$ , and  $a = 0.3$ . Since we want to investigate the effect of the copying process with adding shortcut links on the robustness and the efficiency, we use a small value of  $a$  which is different from 3.0 in the rewiring

algorithm [21]. Too large value of  $a$  restricts linking in the copying process, only the mutual link may be remained at each time step in the growing. This point will be mentioned again in subsection 3.1.

Figures 3(a)-(c) show the degree distributions in the onion-like networks according to DLA, IP, and Eden models. We remark that the largest degree  $k_{max}$  is bounded around 20 with the exponential tail for  $N = 2000$  (see Inset). The load at a node for maintaining links becomes smaller than that in SF networks, since there is no huge hubs. We compare Figs. 3(a)-(c) with the result for the previous generation method of spatial growing networks [23] without the constraint in the surface growth, in which a new node is located on random radius between  $r_{min}$  and  $r_{max}$  with a random direction [39] from the position of a uniformly randomly chosen node in order to make proximity connections heuristically. Figure 3(d) shows the distribution with slightly larger  $k_{max}$  but the exponential tail is more clear in the spatial growing networks without the constraint in the surface growth. The smaller  $k_{max}$  in Fig 3(a)-(c) is probably caused by the constraint.

We show the average degree  $\langle k_{nn} \rangle$  of the nearest neighbor nodes of node with degree  $k$  in Fig. 4. The increasing slope represents positive degree-degree correlations which are necessary to be onion-like topology. The drops in  $k \geq 15$  are ignorable because of finite-size effect (see the tails of  $p(k)$  in Fig. 3). Note that the case of  $\delta = 0.1$  has also positive degree-degree correlations in spite of the tree-like structure without onion-like topology. From top to bottom in Fig. 5, we show examples of tree-like and onion-like topological structures visualized by Pajek [40] in ignoring the spatial positions of nodes on the surface growth. In particular, from the 2nd row to the bottom for  $\delta = 0.3, 0.5, 0.7$ , and 0.9, high degree nodes concentrate on the center area while low degree

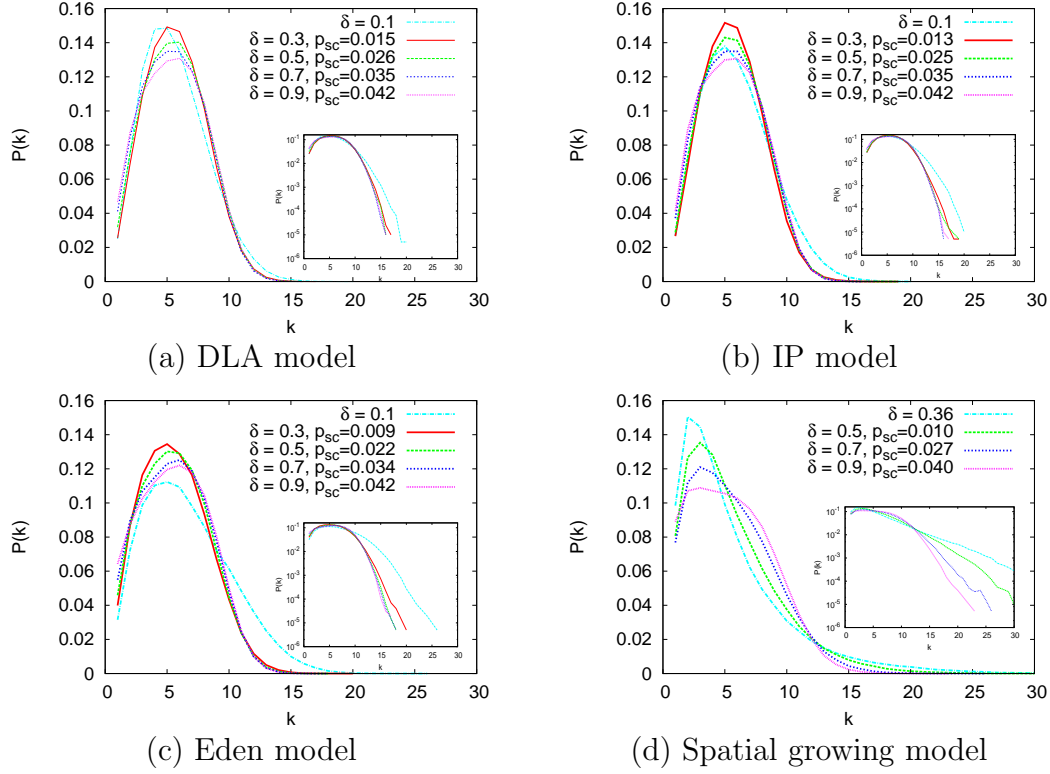


Fig. 3. (Color online) Degree distribution in the networks according to (a) DLA, (b) IP, (c) Eden, and (d) Spatial growing models for  $N = 2000$  with  $\langle k \rangle \approx 5.6$ . Inset shows the exponential decay of tail part approximated by a straight line in semi-log plot. These results are averaged over 100 samples.

nodes surround them.

### 3 Robustness and efficiency on the growing networks

We investigate the robustness against random failures and malicious attacks in subsection 3.1, the growing behavior in subsection 3.2, and the efficiency of path in subsection 3.3. In the malicious attack, nodes are removed in decreasing order of the current degrees through the recalculations [41]. We also discuss the resilience against sequential attacks in subsection 3.4.

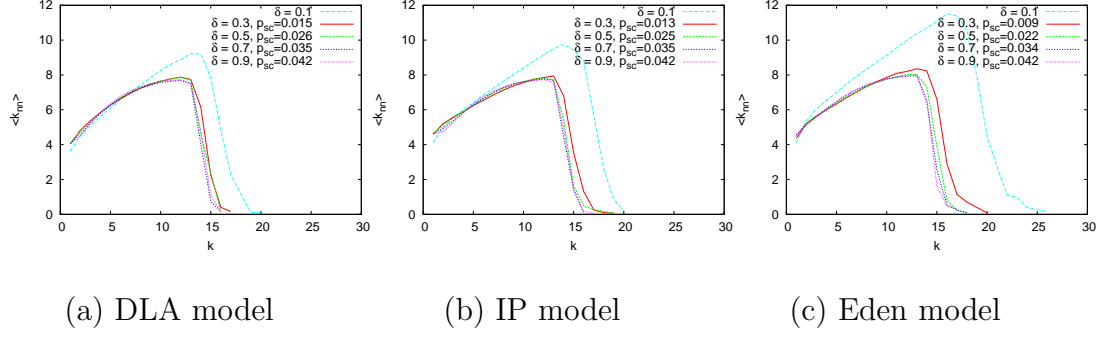


Fig. 4. (Color online) Distribution of the average degree  $\langle k_{nn} \rangle$  of the nearest neighbor nodes of node with degree  $k$  in the networks according to (a) DLA, (b) IP, and (c) Eden models from left to right for  $N = 2000$  with  $\langle k \rangle \approx 5.6$ . Positive degree-degree correlations appear except the tails with finite-size effect in all cases. These results are averaged over 100 samples.

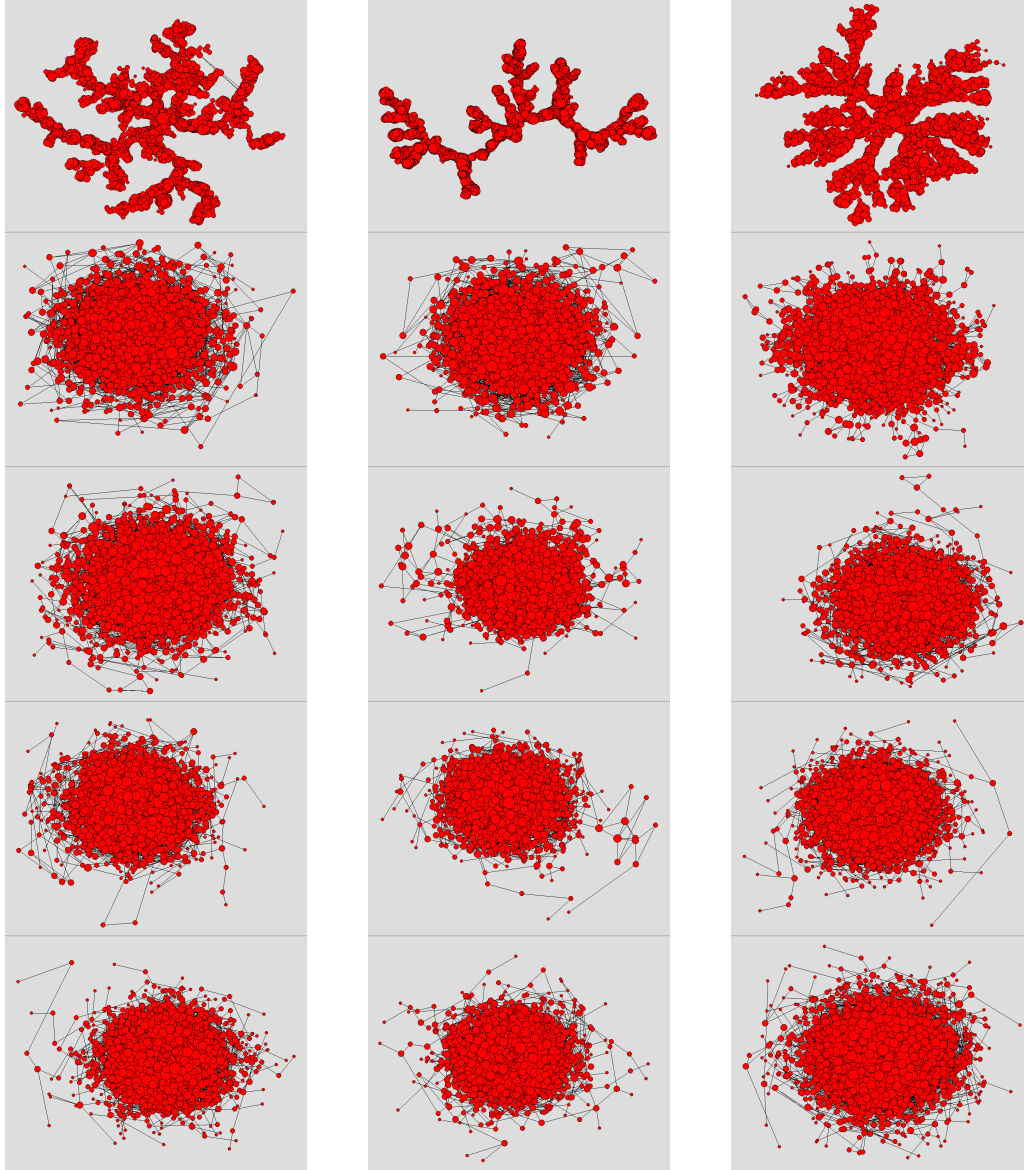
### 3.1 Robustness of connectivity on the growing networks

We consider following two measures for the robustness of connectivity and the degree-degree correlation in a network. For the robustness, we investigate an index [17,18,21]:

$$R = \frac{1}{N} \sum_{q=1/N}^1 S(q), \quad (2)$$

where  $S(q)$  denotes the number of nodes in the giant component (GC: largest connected cluster) after removing  $qN$  nodes,  $q$  is a fraction of removed nodes by random failures or malicious attacks. The range of  $R$  is  $[0, 0.5]$ , where  $R = 0$  corresponds to a completely disconnected network consisting of isolated nodes, and  $R = 0.5$  corresponds to the most robust network. As a measure of degree-degree correlation, we investigate the assortativity [42,43]

$$r = \frac{S_1 S_e - S_2^2}{S_1 S_3 - S_2^2},$$



(a) DLA model

(b) IP model

(c) Eden model

Fig. 5. Visualization of the topological structures of the networks according to (a) DLA, (b) IP, and (c) Eden models from left to right. A tree-like structure appears at the top for  $\delta = 0.1$ , in otherwise onion-like structures with a core area of high degree nodes surrounded by low degree nodes appear from the 2nd row to the bottom for  $\delta = 0.3, 0.5, 0.7$  and  $0.9$ . The node size is proportional to its degree.

where  $S_1 = \sum_i k_i$ ,  $S_2 = \sum_i k_i^2$ ,  $S_3 = \sum_i k_i^3$ ,  $S_e = \sum_{ij} A_{ij} k_i k_j$ ,  $A_{ij}$  denotes the  $i$ - $j$  element of the adjacency matrix. The range of  $r$  is  $[-1, 1]$  as the Pearson correlation coefficient for degrees. Nodes with similar degrees tend to

be connected as  $r > 0$  is larger. Note that onion structure and assortativeness with a large  $r > 0$  are distinct properties [17]: *Not all assortative networks have onion structure but all onion networks are assortative* [21]. Therefore, the value of  $r > 0$  is relatively large in an onion-like network.

Table 1 shows the average values over 100 samples for our networks with  $a = 0.3$  in the 4-6th columns and the corresponding rewired version reconstructed by Wu and Holme's algorithm [21] with  $a = 3.0$  in the 7-9th columns.  $R_{\text{failures}}$  and  $R_{\text{attacks}}$  denote the robustness index defined by Eq. (2) against random failures and malicious attacks, respectively. Note that the rate  $p_{sc}$  of adding shortcut links is regulated to be  $\langle k \rangle \approx 5.6$  with a same connection density. We remark that, with higher values of  $R$ , the robustness is improved from the tree-like network generated by only the copying process for  $\delta = 0.1$  to the networks for  $\delta = 0.3 \sim 0.9$ . These networks have an onion-like topological structure with high assortativity  $r$ , since the values of  $R$  are slightly smaller but almost coincide with  $R = 0.436 \sim 0.444$  against random failures and  $R = 0.307 \sim 0.326$  against malicious attacks in the rewired version [21] to be an onion-like network with the nearly optimal robustness. Although the assortativity  $r$  in the rewired version becomes larger in all cases, the improvement on the robustness from our networks is small. Table 2 shows the results for comparison between the cases of  $a = 0.3$  and  $a = 3.0$ . In order to be  $\langle k \rangle \approx 5.6$  in the case of  $a = 3.0$ , larger rates  $p_{sc}$  are necessary especially for large rates  $\delta$  of deletion. The setting of  $p_{sc}$  means that the effect of the copying process becomes very weak within limited strong degree-degree correlations, because almost all of duplication links are failed as deletion at each time step as similar to the case of  $\delta = 0.9$ . Not surprisingly, a larger assortativity  $r$  is obtained in Table 2 because of stronger degree-degree correlations by larger  $a$  than that



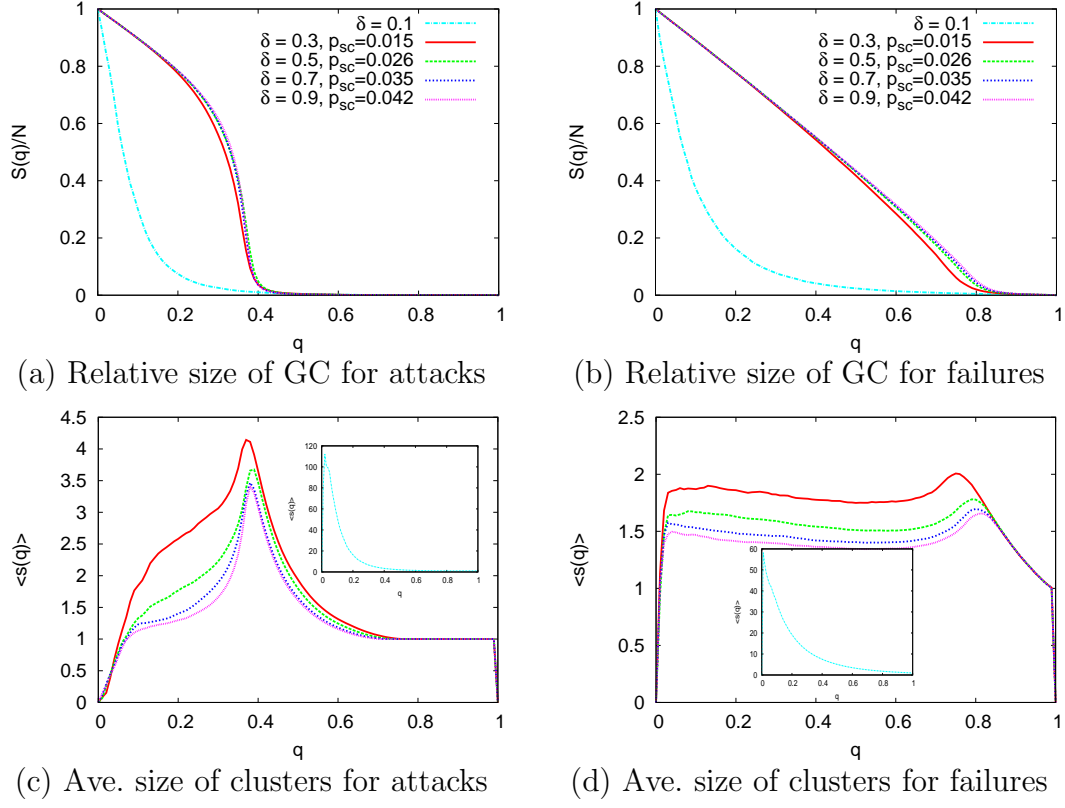


Fig. 6. (Color online) Robustness against (a)(c) malicious attacks and (b)(d) random failures in the networks according to DLA model for  $N = 2000$  with  $\langle k \rangle \approx 5.6$ . The top:(a)(b) shows the relative size  $S(q)/N$  of the giant component (GC) versus fraction  $q$  of removed nodes, and the bottom:(c)(d) shows the average size  $\langle s(q) \rangle$  of isolated clusters except the GC. Similar graphs are obtained for IP and Eden models.

for each corresponding case in Table 1. However, the value of robustness index  $R$  in Table 2 is at a same level as that for each corresponding case in Table 1. There are no notable differences among these results for DLA, IP, Eden models from top to bottom in both Tables. Thus, the setting of  $a = 0.3$  does not lose the intrinsic property for the robustness in our networks, moreover the effect of the copying process remains.

In the following until the end of next section, we set  $a = 0.3$  unless otherwise noted. Figure 6 shows typical results of the robustness. Inset (cyan line) shows

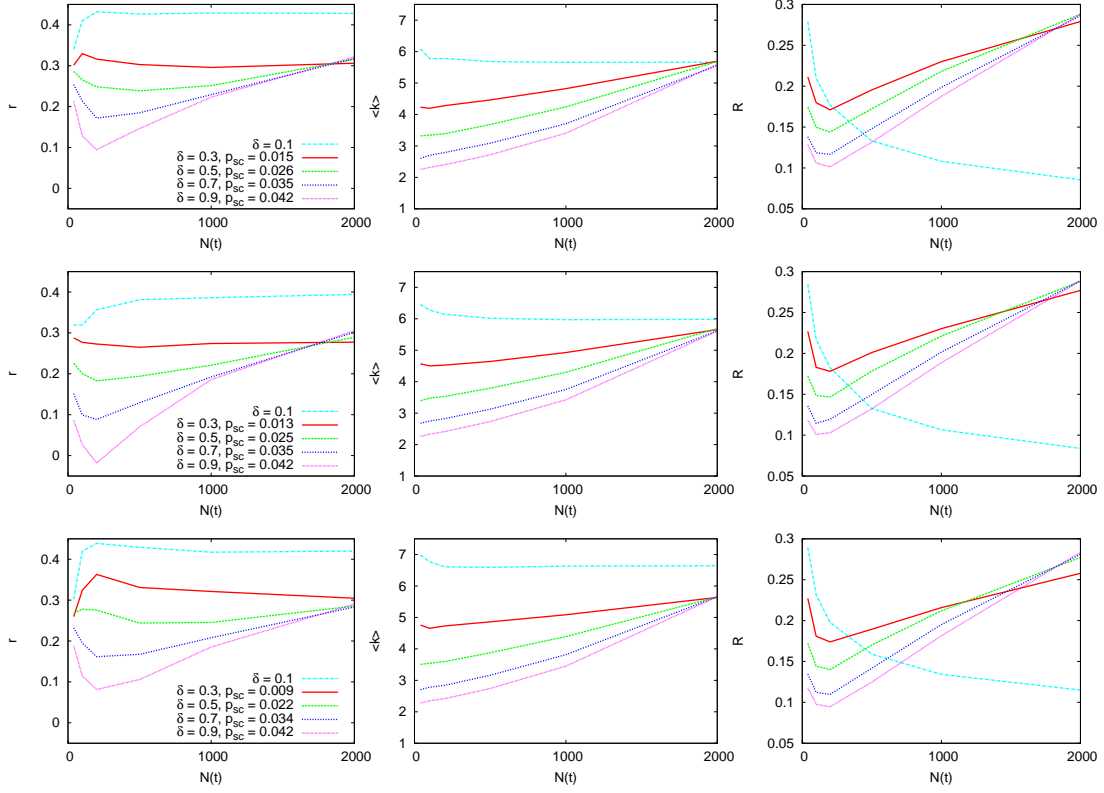


Fig. 7. (Color online) Time-courses of assortativity  $r$ , average degree  $\langle k \rangle$ , robustness index  $R$  against the malicious attacks in the growing networks according to (top) DLA, (middle) IP, (bottom) Eden models for the size  $N(t)$ . These results are averaged over 100 samples.

the vulnerability in the case of tree-like networks for  $\delta = 0.1$ . Note that the value of  $R$  defined by Eq.(2) corresponds to the area under the line of  $S(q)/N$ . The peak of  $\langle s \rangle$  corresponds to the critical point  $q_c$  at the breaking of the GC (dropping point of  $S(q)/N$ ). Although a larger  $q_c$  indicates a more robust network,  $R$  is generally a more precise index than  $q_c$ . Because different values of  $R$  can exist for a same value of  $q_c$  depending on the steepness of dropping curve of  $S(q)/N$ .

### 3.2 Growing behavior

We investigate the growing behavior of our proposed networks. In Fig. 7 left, middle, and right, for the time-courses of assortativity  $r$ , average degree  $\langle k \rangle$ , and robustness index  $R$ , we obtain similar results in the networks according to DLA, IP, and Eden models. They are consistent with the behavior in the spatially growing model [23] without the constraint in the surface growth. As shown at the left of Fig. 7 top, middle, and bottom,  $r$  is almost constant through the growing except the cases of  $\delta = 0.7$  and  $0.9$  denoted by dashed (blue) and dotted (magenta) lines. At the middle column of Fig. 7 top, middle, and bottom,  $\langle k \rangle$  increases for the growing size  $N(t) = t + 4$ . The slope (increasing rate) becomes steeper as the deletion rate  $\delta$  is larger. At the right of Fig. 7 top, middle, and bottom, while  $R$  also increases in the simultaneous progress of the copying and adding shortcut links, it decreases in the cases of  $\delta = 0.1$  without shortcuts in the tree-like network denoted by the dashed (cyan) lines. In general, larger  $\langle k \rangle$  with more links tends to lead to higher robustness. Indeed, the increasing of  $\langle k \rangle$  corresponds to the increasing of  $R$  in Fig. 7 top, middle, and bottom. Note that the decrease of  $R$  in the first stage of small  $N(t)$  is due to the tree-like structure before shaping an onion-like topological structure. Thus, our proposed networks become more robust in the growth with the enhancement of onion-like topology. We remark that the case of  $\delta = 0.1$  seems to be good with high  $R$  in the first stage of small  $N(t)$  while the cases of  $\delta = 0.7$  and  $0.9$  (blue and magenta lines) seem to be good with larger increasing around the last stage of large  $N(t)$ . The case of  $\delta = 0.3$  (red line) is comparatively stable with smaller fluctuation in the entire stage.

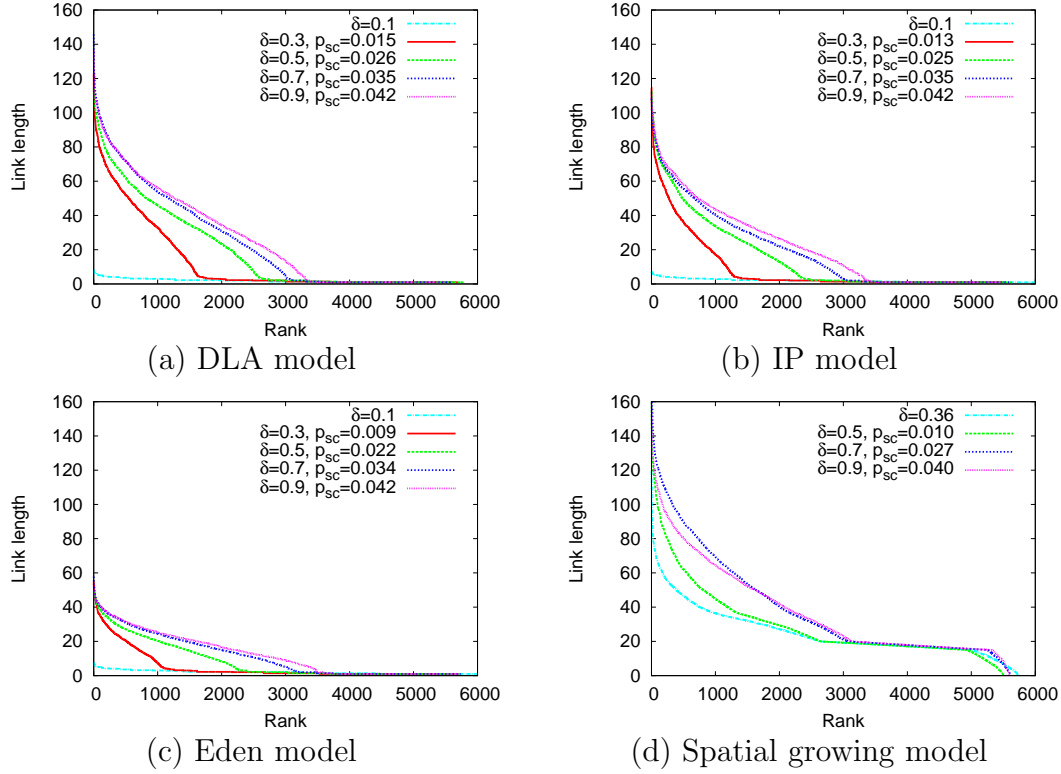
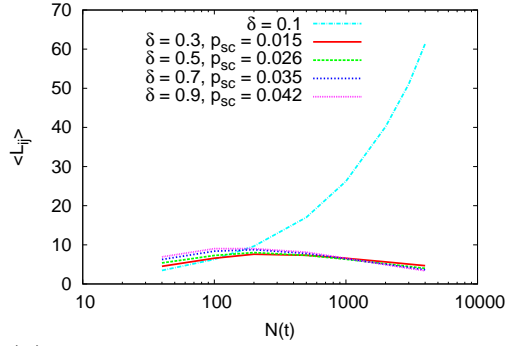


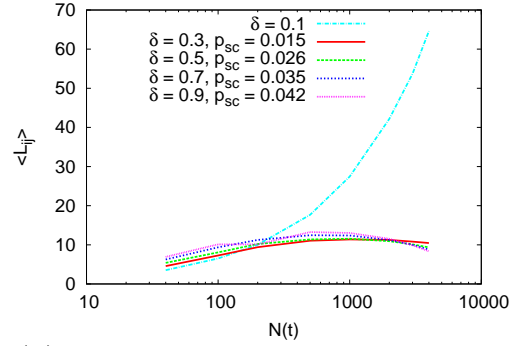
Fig. 8. (Color online) Rank plot of link lengths measured by the Euclidean distance in the networks for  $N = 2000$  with  $\langle k \rangle \approx 5.6$ . These results are averaged over 100 samples.

### 3.3 Efficiency of path on the growing networks

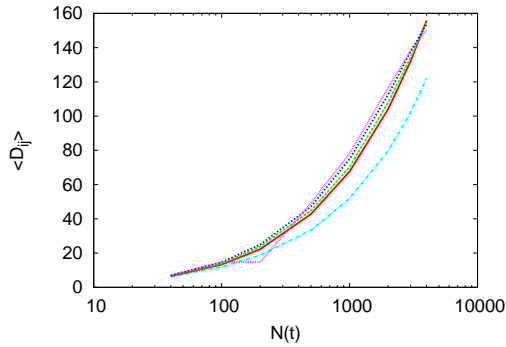
Next, we investigate the communication or transportation efficiency in the growing networks. Obviously, shorter links and paths are better with both less construction and maintenance costs. Figure 8 shows the rank plot of link lengths. The order of shorter links is (c) Eden model < (b) IP model < (a) DLA model < (d) Spatial growing model [23] without the constraint in the surface growth, however the difference between (b) and (a) is very small. This order of link lengths is reasonable because Eden model tends to be compact while IP model tends to percolate making some holes as porous structure and DLA model tends to spread widely along dendritic edges. The tops of Figs. 9, 10, and 11 show the average path length  $\langle L_{ij} \rangle$  counted by hops between two



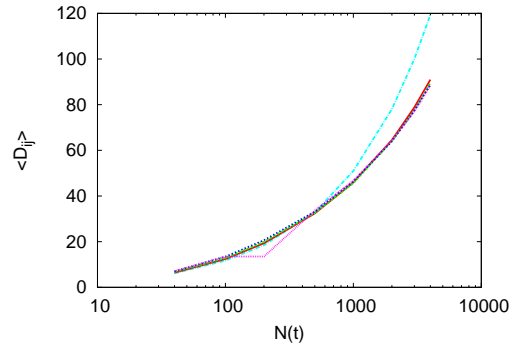
(a) Ave. hops on min. hop paths on the nets according to DLA model



(b) Ave. hops on shortest paths on the nets according to DLA model



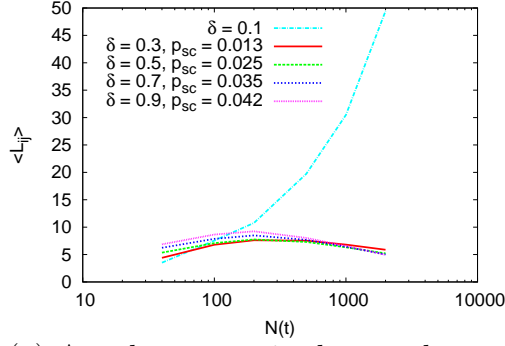
(c) Ave. dist. on min. hop paths on the nets according to DLA model



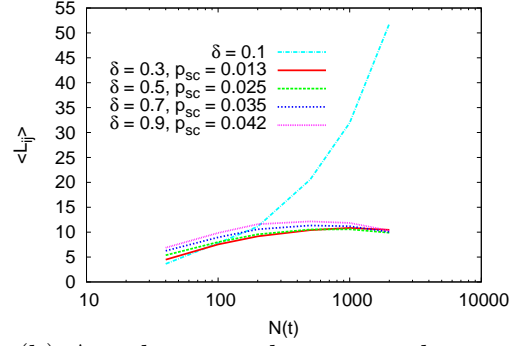
(d) Ave. dist. on shortest paths on the nets according to DLA model

Fig. 9. (Color online) Average path length  $\langle L_{ij} \rangle$  counted by hops (top:(a)(b)) and the average distance  $\langle D_{ij} \rangle$  measured by Euclidean distance (bottom:(c)(d)) in the growing networks according to DLA model. The left:(a)(c) and right:(b)(d) show the results for the minimum hop paths and the shortest distance paths between two nodes, respectively. These results are averaged over 100 samples.

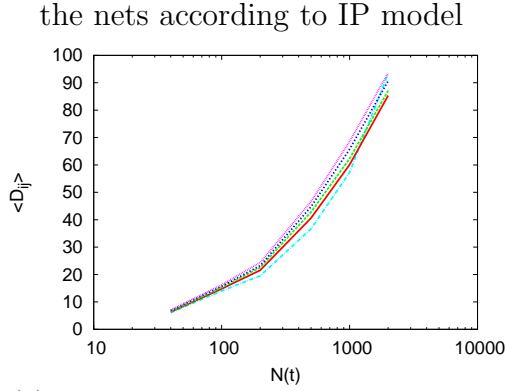
nodes on the paths of (left) minimum hop and (right) shortest distance. We obtain in the tree-like networks (cyan line) monotone increasing curves, while in the onion-like networks (other color lines) convex curves with up-down, whose parts in decreasing the number of hops on both paths are related to the increasing of  $\langle k \rangle$  with more links as shown at the middle column of Fig. 7. It is remarkable that almost constant path length even for the growing size is better than  $O(\log N)$  of the SW property.



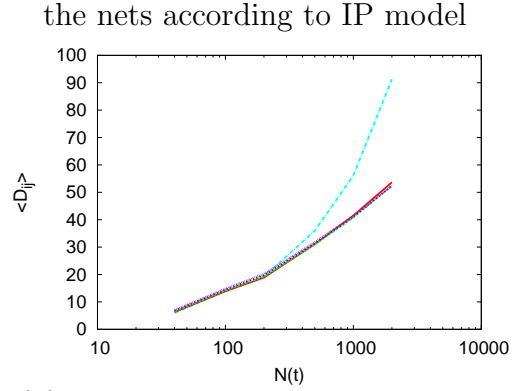
(a) Ave. hops on min. hop paths on



(b) Ave. hops on shortest paths on



(c) Ave. dist. on min. hop paths on



(d) Ave. dist. on shortest paths on

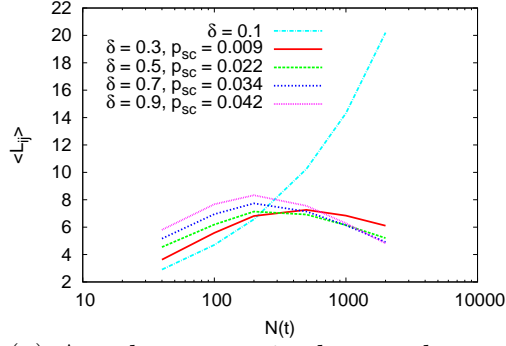
the nets according to IP model

the nets according to IP model

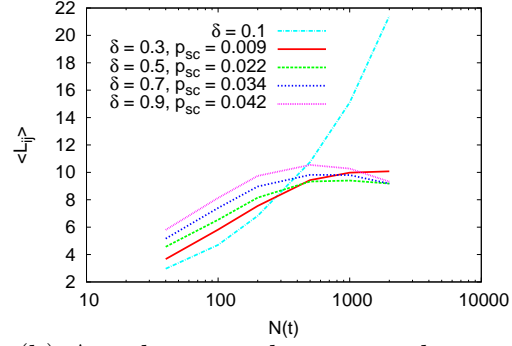
Fig. 10. (Color online) Average path length  $\langle L_{ij} \rangle$  counted by hops (top:(a)(b)) and the distance  $\langle D_{ij} \rangle$  measured by Euclidean distance (bottom:(c)(d)) in the growing networks according to IP model. The left:(a)(c) and right:(b)(d) show the results for the minimum hop paths and the shortest distance paths between two nodes, respectively. These results are averaged over 100 samples.

The bottoms of Figs. 9, 10, and 11 show the average path distance  $\langle D_{ij} \rangle$  measured by the sum of link lengths as Euclidean distances on the paths of (left) minimum hop and (right) shortest distance. We remark that evident difference does not appear in  $\langle D_{ij} \rangle$  for varying  $\delta$  in each of Figs. 9, 10, and 11 except the tree-like networks for  $\delta = 0.1$  (cyan line).

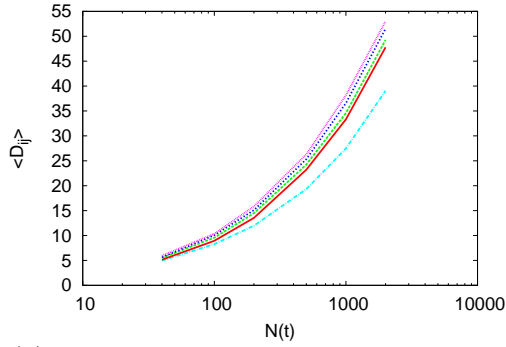
The orders of efficient shorter paths are Fig. 11: Eden model < Fig. 10: IP model < Fig. 9: DLA model in the measures of both  $\langle L_{ij} \rangle$  and  $\langle D_{ij} \rangle$ , however



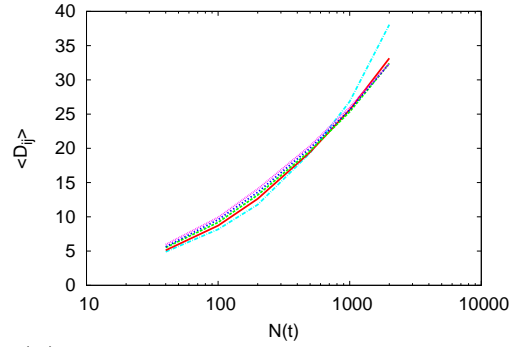
(a) Ave. hops on min. hop paths on the nets according to Eden model



(b) Ave. hops on shortest paths on the nets according to Eden model



(c) Ave. dist. on min. hop paths on the nets according to Eden model



(d) Ave. dist. on shortest paths on the nets according to Eden model

Fig. 11. (Color online) Average path length  $\langle L_{ij} \rangle$  counted by hops (top:(a)(b)) and the distance  $\langle D_{ij} \rangle$  measured by Euclidean distance (bottom:(c)(d)) in the growing network according to Eden model. The left:(a)(c) and right:(b)(d) show the results for the minimum hop paths and the shortest distance paths between two nodes, respectively. These results are averaged over 100 samples.

the difference among them is small especially in  $\langle L_{ij} \rangle$  for  $\delta = 0.3 \sim 0.9$ . In addition, all of them in Figs. 9, 10, and 11 slightly deviate from straight lines of  $O(\log N)$  in semi-log plot as the SW property, although the SW property is obtained in the spatial growing networks [23] without the constraint in the surface growth. Thus, our proposed networks are efficient because the increasing rates of the average path lengths and distances are suppressed in the growing size. Note that the length  $\langle L_{ij} \rangle$  on the minimum hop path (left) is shorter than that on the shortest distance path (right), while the distance

$\langle D_{ij} \rangle$  on the minimum hop path (left) is longer than that on the shortest distance path (right), in each figure.

### 3.4 *Resilient connectivity against sequential attacks*

Through this paper, we discuss dynamics of network configuration itself at the most basic infrastructure for communication or transportation systems, in which temporal and/or fixed (corresponding to wireless and/or wired) connections are possible depending on the time-scale for changing the connection structure in a network. The quick change results in ad hoc networks, while the slow change is treated as an incremental modification of network. Both cases and the mixed one are not excluded, however we have assumed that each node or link is persisted once it is added unless removed by failures or attacks to simplify the discussion. While other dynamics of information flows, rumor spreading, opinion formation, synchronization, or logistics on a network, is significant for applications in wireless, sensor, mobile communication systems or autonomous transportation systems, in which operation protocols for birth and death of communication or transportation request, routing, avoidance of congestion, task allocation, queuing, awareness of location, monitoring of system's states or conditions, and so on [44], are necessary. We have pointed out the issues of rethinking packet generation according to population, decentralized routing strategy, and link hierarchy among long and short ranges with high and low transfer speeds [45] in the state-of-the-art network technologies. In addition, although several models have been proposed for the coevolution of network formation and opinion spreading [46,47] and for the coupled dynamics with network evolution and packet flows [6,7,48,49,50], they are beyond



our current scope because of more complex dynamics between network generation and information flow in various protocols, device technologies, users, and situations of utilization.

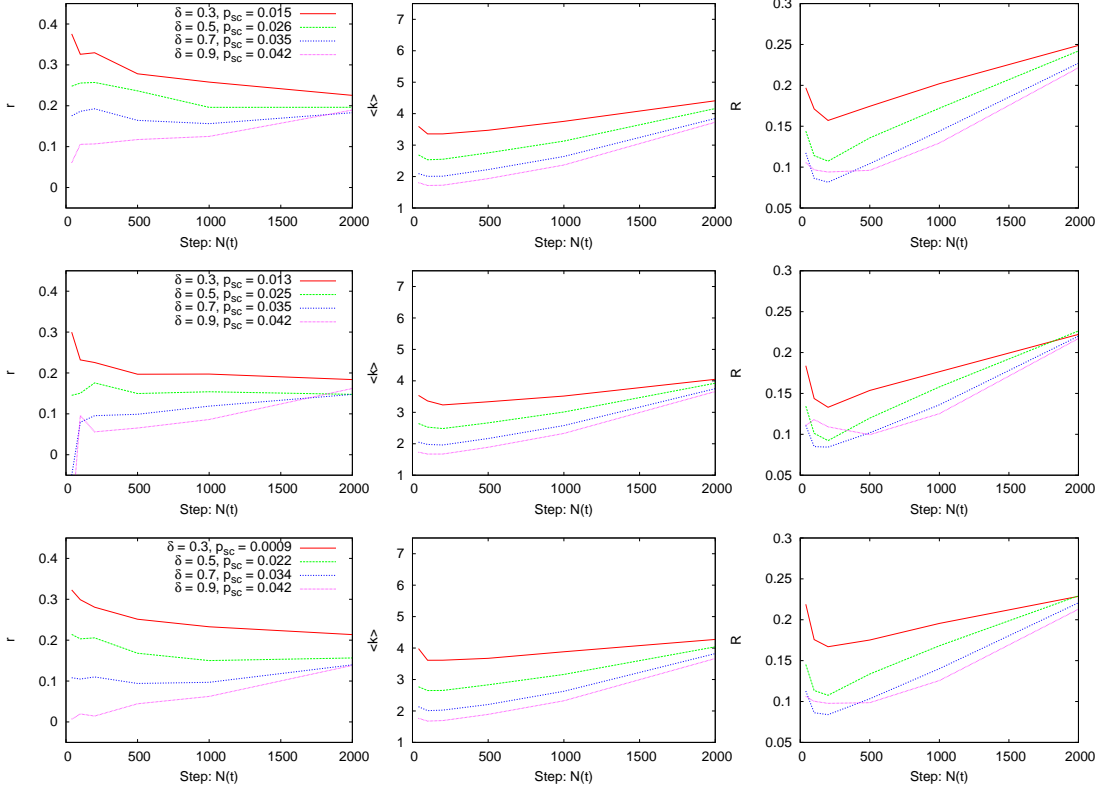


Fig. 12. (Color online) Time-courses of assortativity  $r$ , average degree  $\langle k \rangle$ , robustness index  $R$  against the malicious attacks in the networks damaged by sequential attacks at every 10 time steps. These results are averaged over 100 samples according to (top) DLA, (middle) IP, (bottom) Eden models.

On the other hand, we consider an interaction of network generation with a change of environment, especially in sequential attacks. We show that our proposed networks have resilient connectivity even in the previously described growing scheme of constant  $\delta$ ,  $p_{sc}$ , and  $IT$ , without any remedial measures for insistent attacks. Figure 12 shows the time-courses of  $r$ ,  $\langle k \rangle$ , and  $R$  against the further attacks in the networks damaged by sequential attacks. We set the same values of  $\delta$ ,  $p_{sc}$ , and  $IT$  in the previous subsection, and the largest

degree node with its links is removed through the recalculation of degrees at every 10 time steps. At the left of Fig. 12 top, middle, and bottom for DLA, IP, and Eden models, respectively, the damaged networks by the sequential attacks have positive degree-degree correlations around  $r \approx 0.2$  somehow or other. At the middle and right of Fig. 12, the robustness is recovered with slowly increasing  $\langle k \rangle$ , since  $R$  is decreasing in the first stage of small  $N(t)$  but increasing after a time. We obtain similar behavior in these spatial growth models as shown in Fig. 12 from top to bottom, and the case of  $\delta = 0.3$  (red line) with the stronger effect of the copying is better than other cases of  $\delta = 0.5, 0.7$ , and  $0.9$  (green, blue, and magenta lines). In particular, in the case of  $\delta = 0.9$  (magenta line),  $R$  does not increase until  $N(t) \approx 500$  due to the insistent attacks. All values of  $r$ ,  $\langle k \rangle$ , and  $R$  in Fig. 12 are smaller, as compared with the results for the pure growing networks in Fig. 7. Thus, even the damaged networks maintain the robust onion-like topology in the growing scheme. We remark that in the sequential attacks the robustness is protected locally by the copying, and enhanced globally in connecting isolated clusters by adding shortcut links between randomly chosen nodes. Remember the local proxy and complementary functions in subsection 2.1. When more severe attacks in shorter interval at every 5 time steps are given, around the robustness index  $R \approx 0.15 \sim 0.2$  against the further attacks, the networks no longer have an onion-like topological structure because of the assortativity  $r \approx 0.0$  or  $r < 0.0$  in this growing scheme of constant  $\delta$ ,  $p_{sc}$ , and  $IT$  without any remedial measures.

## 4 Conclusion

We have proposed a spatial design method of robust and efficient networks with typical surface growth patterns. It is self-organized through the simultaneous progress of the copying and adding shortcut links [23] taking into account linking homophily to make an onion-like topological structure with positive degree-degree correlations. For the copying, the selection of node is not uniformly at random but limited to the neighbors of the perimeter of connected cluster in the growing network on a space. In spite of the constraint on the surface growth, we have obtained that the robustness against random failures and malicious attacks is nearly optimal or slightly weaker than the entirely rewired version [21]. Moreover, the efficiency of path measured in the hop count is better than  $O(\log N)$  of the SW property but one measured in the Euclidean distance slightly degraded from the SW property. In particular, the growing network becomes more robust and efficient in time-course. However, we may have to consider a resource allocation problem for the increasing of  $\langle k \rangle$  required with more links. On the other hand, we have also found that there are no huge hubs bounded by an exponential tail of degree distribution, and that large degree nodes are spontaneously interspersed on a space.

Moreover, we have shown that the robust onion-like topological structure remains even in the random growth damaged by the sequential attacks. When a node is removed by serious disasters or insistent attacks, more effective strategies than a constant random growth can be considered to repair the damaged parts. If a new node is added near the removed node as the proxy of it instead of the random location on a neighbor site on the perimeter in the surface growth, the network is probably more effectively healed over. If the param-

ters of  $\delta$ ,  $p_{sc}$ , and  $IT$  are regulated according to the damages, the network is recovered to the original level of performance for the communication or the transportation. These trials will require further study with healing and recovering processes, e.g. we should consider which parts of network have priorities to prevent spreading damages in topological and spatial importance. In a realistic situation such as disaster or battle-field, resources for the strategies are limited and should be allocated effectively in the priorities.

In summary, our growing network models suggest that robust and efficient onion-like topological structure can emerge even when the positions of nodes are limited in the contact area of the spatial network. In the cooperative growing mechanism, the local proxy and complementary robust functions by the copying and adding shortcut links will be useful for temporal evolution of resilient network and a repair strategy in large-scale disasters or system crises. However, it is an issue in general what type of constraint for locating nodes on a space is an obstacle to the emergence of onion-like topology. It may be related to limited facilities from geographical and economical viewpoints.

## Acknowledgment

The author would like to thank Mitsugu Matsushita for his valuable comments about fractal growth models on a space and to anonymous reviewers for their suggestions to improve the readability of manuscript. This research is supported in part by a Grant-in-Aid for Scientific Research in Japan, No. 25330100.

## References

- [1] F. Dressler, *Self-Organization in Sensor and Actor Networks*, John Wiley & Sons, 2007.
- [2] A.-L. Babarási, R. Albert, *Science* 286 (1999) 509–512.
- [3] R. V. Sole, R. Pastor-Satorras, E. Smith, T. B. Kepler, *Advances in Complex Systems* 5 (1) (2002) 43–54.
- [4] R. Pastor-Satorras, E. Smith, R. V. Sole, *Journal of Theoretical Biology* 222 (2) (2003) 199–210.
- [5] D. Helbing, J. Keltsch, P. Molnár, *Nature* 388 (1997) 47–50.
- [6] A. Tero, S. Takagi, T. Saigusa, K. Ito, D. P. Bebber, M. D. Fricker, K. Yumiki, R. Kobayashi, T. Nakagaki, *Science* 327 (5964) (2010) 439–442.
- [7] Y. Hayashi, Y. Megumo, *Physica A* 391 (2012) 872–879.
- [8] J. P. K. Doye, C. P. Massen, *Physical Review E* 71 (2005) 016128.
- [9] T. Zhou, G. Yan, B.-H. Wang, *Physical Review E* 71 (2005) 046141.
- [10] W. Nagel, J. Mecke, J. Ohser, V. Weiss, *Image Analysis & Stereology* 27 (2) (2008) 73–78.
- [11] Y. Hayashi, *Advances in Complex Systems* 12 (1) (2009) 73–86.
- [12] Y. Hayashi, *Physica A* 388 (1) (2007) 991–998, corrigendum (2011).  
<http://www.sciencedirect.com/science/article/pii/S0378437112002592>
- [13] P. L. Krapivsky, S. Redner, E. Ben-Naim, *A Kinetic View of Statistical Physics*, Cambridge University Press, 2010.
- [14] M. J. Alava, S. Dorogovtsev, *Physical Review E* 71 (2005) 036107.

- [15] D. J. Watts, S. H. Strogatz, *Nature* 393 (1998) 440–442.
- [16] R. Albert, H. Jeong, A.-L. Barabási, *Nature* 406 (2000) 36–44.
- [17] C. M. Schneider, A. A. Moreira, J. S. Andrade Jr., S. Havlin, H. J. Herrmann, *PNAS* 810 (10) (2011) 3838–3841.
- [18] H. J. Herrmann, C. M. Schneider, A. A. Moreira, J. S. Andrade Jr., S. Havlin, *Journal of Statistical Mechanics* (2011) P01027.
- [19] T. Tanizawa, S. Havlin, H. E. Physical Review E 85 (2012) 046109.
- [20] C. I. N. S. Filho, A. A. Moreira, R. F. S. Andrade, H. J. Herrmann, J. S. Andrade Jr., *Scientific Report* 5 (9082).  
[www.nature.com/articles/srep09082](http://www.nature.com/articles/srep09082)
- [21] Z.-X. Wu, P. Holme, *Physical Review E* 81 (2011) 026116.
- [22] M.E.J. Newman, S.H. Strogatz, D.J. Watts, *Physical Review E* 64 (2001) 026118.
- [23] Y. Hayashi, *IEEE Xplore Digital Library Proc. of 2014 IEEE 8th Int. Conf. on SASO: Self-Adaptive and Self-Organizing Systems* (2014) 50–59,  
<http://arxiv.org/abs/1411.7719>.
- [24] A. Zolli, A. M. Healy, *Resilience: Why Things Bounce Back*, Simon & Schuster, 2013.
- [25] C. M. Schneider, N. Yazdani, N.A.M. Araújo, S. Havlin, H.J. Herrmann, *Scientific Reports* 3 (2013) 1969. <http://www.nature.com/articles/srep01969>
- [26] M. Stippinger, J. Kertész, *Physica A* 416 (2014) 431–487.
- [27] X.-H. Yanga, S.-L. Lou, G. Chen, S.-Y. Chen, W. Huang, *Physica A* 392 (2013) 3531–3536.
- [28] E. R. Colman, G. J. Rodgers, *Physica A* 392 (2013) 5501–5510.

- [29] M. E. Newman, C. Moore, D. J. Watts, Physical Review Letters 84 (2000) 3201.
- [30] Y. Hayashi, J. Matsukubo, Physica A 380 (2007) 552–562.
- [31] Y. Hayashi, Y. Ono, Physical Review E 82 (2010) 016108.
- [32] D. S. Callaway, J. E. Hopcroft, J. M. Kleinberg, M. E. J. Newman, S. H. Strogatz, Physical Review E 64 (2001) 041902.
- [33] P. Meakin, Fractals, scaling and growth far from equilibrium, Cambridge University Press, 1998.
- [34] E. Ben-Jacob, Contemporary Physics 38 (3) (1997) 205–241.
- [35] D. Wilkinson, J. F. Willemsen, Journal of Physics A: Mathematical and General 16 (1983) 3365–3376.
- [36] H. E. Stanley, A. Coniglio, S. Havlin, J. Lee, S. Schwarzer, M. Wolf, Physica A 205 (1994) 254–271.
- [37] T. A. Witten, L. M. Sander, Physical Review B 27 (9) (1983) 36–44.
- [38] M. Eden, A two-dimensional growth process, in: J. Neyman (Ed.), Proceedings of the 4th Berkeley Symposium on Mathematical Statistics and Probability, Vol. IV of IV, 1961, pp. 223–239.
- [39] R. Xulvi-Brunet, I. M. Sokolov, Physical Review E 75 (2007) 46117.
- [40] <http://vlado.fmf.uni-lj.si/pub/networks/pajek/>
- [41] P. Holme, B. J. Kim, C. N. Yoon, S. K. Han, Physical Review E 65 (2002) 056109.
- [42] M. E. Newman, Physical Review Letters 89 (20) (2003) 208701.
- [43] M. E. Newman, Networks -An Introduction-, Vol. 68, Oxford University Press, New York, NY, 2010.

- [44] M. Barbeau, E. Kranakis, Principles of Ad-hoc Networking, John Wiley & Sons, 2007.
- [45] Y. Hayashi, Rethinking of communication requests, routing, and navigation hierarchy on complex networks -for a biologically inspired efficient search on a geographical space-, in: I. Bilogrevic, A. Rezazadeh, L. Momeni (Eds.), Networks -Emerging Topics in Computer Science, iConcept Press, 2012, Chapter 4, pp. 67–88.  
<https://www.iconceptpress.com/book/networks--emerging-topics-in-computer-science/110000>
- [46] P. Holme, M. E. Newman, Physical Review E 74 (2006) 056108.
- [47] S. Gil, D. H. Zanette, Physics Letters A 356 (2) (2006) 89–94.
- [48] S.-W. Kim, J. D. Noh, Physical Review Letters 100 (2008) 118702.
- [49] S.-W. Kim, J. D. Noh, Physical Review E 80 (2009) 026119.
- [50] Q. Xuan, F. Du, T.-J. Wu, G. Chen, Physical Review E 80 (2010) 046116.



Table 1

Average values over 100 samples in the networks for  $N = 2000$  on the surface growth according to DLA, IP, and Eden models from top to bottom. The 4-6th columns show the results for our networks with  $a = 0.3$ , and the 7-9th columns show the results for the corresponding rewired version [21] with  $a = 3.0$  from our networks with  $a = 0.3$ .

DLA			our	networks	with $a = 0.3$	rewired	version	with $a = 3.0$
$\delta$	$p_{sc}$	$\langle k \rangle$	$r$	$R$ :failures	$R$ :attacks	$r$	$R$ :failures	$R$ :attacks
0.1	0.0	5.663790	0.428085	0.11414846	0.08546072	0.570401	0.44257568	0.32097051
0.3	0.015	5.693130	0.306182	0.42286182	0.27909878	0.563234	0.44446583	0.32624905
0.5	0.026	5.683880	0.315288	0.43330392	0.28798839	0.566574	0.44266511	0.32195528
0.7	0.035	5.560350	0.317886	0.43543737	0.28620190	0.568082	0.43890241	0.31470397
0.9	0.042	5.592120	0.321879	0.43776842	0.28822588	0.573602	0.43836274	0.31299371
IP			our	networks	with $a = 0.3$	rewired	version	with $a = 3.0$
$\delta$	$p_{sc}$	$\langle k \rangle$	$r$	$R$ :failures	$R$ :attacks	$r$	$R$ :failures	$R$ :attacks
0.1	0.0	5.980630	0.394308	0.11528832	0.08374447	0.577101	0.44597737	0.32535835
0.3	0.013	5.656150	0.277479	0.41909362	0.27702885	0.561372	0.44345529	0.32521399
0.5	0.025	5.691770	0.289450	0.4337521	0.28823022	0.569636	0.44294242	0.32367072
0.7	0.035	5.616860	0.301741	0.43641043	0.28870629	0.574130	0.44029968	0.31788086
0.9	0.042	5.606670	0.305765	0.43796751	0.28855921	0.571790	0.43886147	0.31492539
Eden			our	networks	with $a = 0.3$	rewired	version	with $a = 3.0$
$\delta$	$p_{sc}$	$\langle k \rangle$	$r$	$R$ :failures	$R$ :attacks	$r$	$R$ :failures	$R$ :attacks
0.1	0.0	6.644020	0.420114	0.19868989	0.11501878	0.600332	0.45091269	0.33193373
0.3	0.009	5.635930	0.304668	0.41034536	0.25781734	0.567774	0.439060744	0.31314427
0.5	0.022	5.648480	0.285373	0.43086621	0.27727353	0.568454	0.43895619	0.31237012
0.7	0.034	5.657810	0.283205	0.43680778	0.28117685	0.572352	0.43777281	0.30982738
0.9	0.042	5.658680	0.290042	0.43891585	0.28344713	0.566763	0.43673314	0.30796406

Table 2

Average values over 100 samples in the networks for  $N = 2000$  on the surface growth according to DLA, IP, and Eden models from top to bottom. The 4-6th columns show the results for comparison between the cases of  $a = 0.3$  and  $a = 3.0$  that is different parameter setting form Table 1, and the 7-9th columns show the results for the corresponding rewired version [21] with  $a = 3.0$  from our networks with  $a = 3.0$ .

DLA			our	networks	with $a = 3.0$	rewired	version	with $a = 3.0$
$\delta$	$p_{sc}$	$\langle k \rangle$	$r$	$R$ :failures	$R$ :attacks	$r$	$R$ :failures	$R$ :attacks
0.1	0.0	2.834040	0.437167	0.04345627	0.03607689	0.437008	0.32199987	0.18107685
0.3	0.035	5.650160	0.457448	0.43313566	0.2979080	0.583822	0.43888272	0.31681199
0.5	0.039	5.629190	0.457572	0.43389278	0.29740136	0.579910	0.43849948	0.31413023
0.7	0.043	5.594100	0.453034	0.43468667	0.29602458	0.585048	0.43675333	0.31164826
0.9	0.045	5.651210	0.454004	0.43586855	0.29712904	0.582588	0.43772334	0.31261318
IP			our	networks	with $a = 3.0$	rewired	version	with $a = 3.0$
$\delta$	$p_{sc}$	$\langle k \rangle$	$r$	$R$ :failures	$R$ :attacks	$r$	$R$ :failures	$R$ :attacks
0.1	0.0	2.970500	0.400235	0.04522621	0.03565373	0.435406	0.33601715	0.19365666
0.3	0.034	5.635630	0.436601	0.43351504	0.29754534	0.581092	0.43953115	0.31804051
0.5	0.038	5.561670	0.430161	0.43346665	0.29522308	0.582158	0.43758882	0.3138613
0.7	0.043	5.601620	0.430950	0.4351622	0.29589068	0.582668	0.43698282	0.31191742
0.9	0.045	5.662410	0.437168	0.43656923	0.2982953	0.585400	0.43781393	0.31344812
Eden			our	networks	with $a = 3.0$	rewired	version	with $a = 3.0$
$\delta$	$p_{sc}$	$\langle k \rangle$	$r$	$R$ :failures	$R$ :attacks	$r$	$R$ :failures	$R$ :attacks
0.1	0.0	3.167770	0.384913	0.07280454	0.0402646	0.445969	0.35275171	0.19681491
0.3	0.032	5.666700	0.425713	0.43319376	0.29233634	0.580907	0.43759013	0.31193571
0.5	0.037	5.629740	0.422828	0.4342548	0.29071317	0.582505	0.43608627	0.3089480
0.7	0.043	5.663520	0.419765	0.43617703	0.29168745	0.582820	0.43608627	0.30800115
0.9	0.045	5.664820	0.420572	0.43666387	0.2916347	0.579751	0.43535101	0.30689578